AMERICAN SOCIETY FOR MICROBIOLOGY | Journal of Virology®

GENETIC DIVERSITY AND EVOLUTION

Plasticity of Amino Acid Residue 145 Near the Receptor Binding Site of H3 Swine Influenza A Viruses and Its Impact on Receptor Binding and Antibody Recognition

Jefferson J. S. Santos,[a] Eugenio J. Abente,[b] Adebimpe O. Obadan,[a] Andrew J. Thompson,[c] Lucas Ferreri,[a] Ginger Geiger,[a] Ana S. Gonzalez-Reiche,[a,d] Nicola S. Lewis,[e] David F. Burke,[f] Daniela S. Rajão,[a] James C. Paulson,[c] Amy L. Vincent,[b] Daniel R. Perez[a]

[a]Department of Population Health, Poultry Diagnostic and Research Center, University of Georgia, Athens, Georgia, USA
[b]Virus and Prion Research Unit, National Animal Disease Center, Agricultural Research Service, U.S. Department of Agriculture, Ames, Iowa, USA
[c]Department of Molecular Medicine and Immunology & Microbiology, The Scripps Research Institute, La Jolla, California, USA
[d]Department of Genetics and Genomic Sciences, Icahn School of Medicine at Mount Sinai, New York, New York, USA
[e]Department of Pathobiology and Population Sciences, Royal Veterinary College, Hatfield, Hertfordshire, United Kingdom
[f]Department of Zoology, University of Cambridge, Cambridge, United Kingdom

ABSTRACT The hemagglutinin (HA), a glycoprotein on the surface of influenza A virus (IAV), initiates the virus life cycle by binding to terminal sialic acid (SA) residues on host cells. The HA gradually accumulates amino acid substitutions that allow IAV to escape immunity through a mechanism known as antigenic drift. We recently confirmed that a small set of amino acid residues are largely responsible for driving antigenic drift in swine-origin H3 IAV. All identified residues are located adjacent to the HA receptor binding site (RBS), suggesting that substitutions associated with antigenic drift may also influence receptor binding. Among those substitutions, residue 145 was shown to be a major determinant of antigenic evolution. To determine whether there are functional constraints to substitutions near the RBS and their impact on receptor binding and antigenic properties, we carried out site-directed mutagenesis experiments at the single-amino-acid level. We generated a panel of viruses carrying substitutions at residue 145 representing all 20 amino acids. Despite limited amino acid usage in nature, most substitutions at residue 145 were well tolerated without having a major impact on virus replication *in vitro*. All substitution mutants retained receptor binding specificity, but the substitutions frequently led to decreased receptor binding. Glycan microarray analysis showed that substitutions at residue 145 modulate binding to a broad range of glycans. Furthermore, antigenic characterization identified specific substitutions at residue 145 that altered antibody recognition. This work provides a better understanding of the functional effects of amino acid substitutions near the RBS and the interplay between receptor binding and antigenic drift.

IMPORTANCE The complex and continuous antigenic evolution of IAVs remains a major hurdle for vaccine selection and effective vaccination. On the hemagglutinin (HA) of the H3N2 IAVs, the amino acid substitution N 145 K causes significant antigenic changes. We show that amino acid 145 displays remarkable amino acid plasticity *in vitro*, tolerating multiple amino acid substitutions, many of which have not yet been observed in nature. Mutant viruses carrying substitutions at residue 145 showed no major impairment in virus replication in the presence of lower receptor binding avidity. However, their antigenic characterization confirmed the impact of the 145 K substitution in antibody immunodominance. We provide a better understanding of the functional effects of amino acid substitutions implicated in antigenic drift and its consequences for receptor binding and antigenicity. The mutation anal-

Citation Santos JJS, Abente EJ, Obadan AO, Thompson AJ, Ferreri L, Geiger G, Gonzalez-Reiche AS, Lewis NS, Burke DF, Rajão DS, Paulson JC, Vincent AL, Perez DR. 2019. Plasticity of amino acid residue 145 near the receptor binding site of H3 swine influenza A viruses and its impact on receptor binding and antibody recognition. J Virol 93:e01413-18. https://doi.org/10.1128/JVI.01413-18.

Editor Adolfo García-Sastre, Icahn School of Medicine at Mount Sinai

Address correspondence to Daniel R. Perez, dperez1@uga.edu.

Received 16 August 2018
Accepted 13 October 2018
Accepted manuscript posted online 24 October 2018
Published 4 January 2019

yses presented in this report represent a significant data set to aid and test the ability of computational approaches to predict binding of glycans and in antigenic cartography analyses.

KEYWORDS H3 subtype, hemagglutinin, influenza vaccines, swine influenza, virus evolution

The surface hemagglutinin (HA) glycoprotein of influenza A virus (IAV) has a pivotal role in initiating the virus life cycle by binding to the virus receptor on target cells. HA binds to sialic acid (SA) residues that occur as terminal monosaccharides in glycoproteins and glycolipids on the cell surface. SA receptors engaged by IAV are linked to galactose (Gal) in an α2-3 (SAα2-3Gal) or α2-6 (SAα2-6Gal) linkage configuration (1). Located in a small depression on the globular head of HA, the receptor binding site (RBS) is composed of the 130-loop, the 150-loop, the 190-helix, and the 220-loop. A series of conserved residues, including Tyr98, Ser136, Trp153, and His183 (H3 numbering), forms the base of the RBS and is important for SA interaction (2, 3). Although some HA residues on the RBS are critical for receptor specificity (4–6), other residues may influence binding by modulating virus-receptor binding avidity (7, 8).

IAV remains an important pathogen for humans and swine (9). While influenza vaccines are commercially available, the relative effectiveness of these vaccines is heavily dependent on the antigenic match of vaccine strains to circulating virus strains (10, 11). Most of the humoral immune response elicited by influenza vaccination or natural exposure is directed against HA to block virus infection (12, 13). Through a mechanism known as antigenic drift, IAV can circumvent the preexisting antibody response by generating genetic variants during replication with amino acid substitutions in key HA epitopes on the globular head, allowing for the emergence of escape mutant viruses (14). Antigenic drift is a frequent cause of reduced vaccine effectiveness, especially for H3N2 IAVs (15).

Defining the molecular basis of antigenic drift has important implications for understanding IAV evolution and has been facilitated by methodological advances, such as antigenic cartography (16). A recent study identified seven residues (residues 145, 155, 156, 158, 159, 189, and 193) on the globular head of the HA as the major determinants of antigenic drift during the evolution of human H3N2 IAVs (17). Interestingly, all seven residues were located adjacent to the RBS (17), and these residues therefore may also influence receptor binding. The importance of this small set of HA residues as major drivers of antigenic evolution has been demonstrated for IAVs circulating in other hosts, including swine H3N2 IAVs (18).

Antigenic changes in human H3N2 IAVs over the course of time were shown to be frequently caused by a single amino acid substitution in one of the seven residues, with specific substitutions involved in antigenic change more than once (17). One of those substitutions, N 145 K, was shown in two separate instances to be the major determinant of antigenic drift during the evolution of human H3N2 IAVs (16, 17). While there is evidence that N 145 K caused large antigenic changes (7, 16–18) and also altered receptor binding avidity (7), it remains unclear whether there are functional constraints to substitutions at residue 145 or how alternative amino acid substitutions at this residue may affect receptor binding and antigenic properties.

In the present study, we carried out site-directed mutagenesis to prepare a panel of H3 HA mutant viruses carrying a single amino acid substitution at residue 145 and subsequently evaluated the impact of substitutions at this key HA residue on receptor binding and antibody recognition. Our data indicate that residue 145 displayed remarkable amino acid plasticity *in vitro*, tolerating multiple amino acid substitutions, many of which have not yet been observed in nature. Mutant viruses carrying substitutions at residue 145 showed no major impairment in virus replication. While all substitution mutants retained binding to SAα2-6Gal glycans compared to the wild type, mutant viruses with substitutions not commonly found in nature displayed diminished receptor binding capacity. Antigenic characterization confirmed the impact of HA

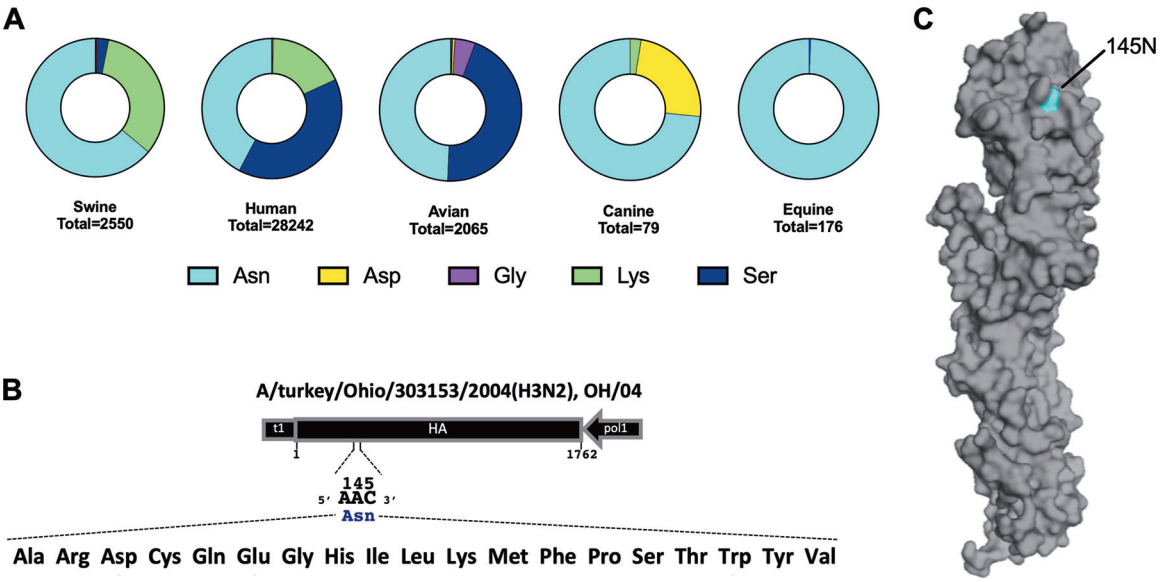

FIG 1 Amino acid plasticity at residue 145. (A) Publicly available H3 HA sequences were retrieved, and the relative frequencies of identified amino acids at residue 145 were calculated for swine, human, avian, canine, and equine AIVs. Amino acids present at frequency below 1% are not labeled in the figure. (B) Schematic representation of the HA gene segment of A/turkey/Ohio/313053/2004 (H3N2), depicting the codon corresponding to residue 145 and respective amino acid substitutions introduced by site-directed mutagenesis. (C) HA monomeric structure of A/turkey/Ohio/313053/2004 (H3N2), indicating the location of HA residue 145.

residue 145 K in antibody immunodominance. These findings have important implications for understanding virus evolution and aiding the development of novel vaccine design approaches.

RESULTS

HA residue 145 displays remarkable amino acid plasticity *in vitro*. The HA N 145 K substitution results in significant antigenic changes in both human and swine H3N2 IAVs (7, 16–18). Asparagine (Asn or N) was the most prevalent amino acid found at residue 145 across all analyzed hosts (Fig. 1A). In swine-origin IAVs, around 64% of isolates possessed Asn at residue 145, followed by lysine (Lys or K) at ~33% and serine (Ser or S) at ~2.5%. In human-origin IAVs, about 42% of isolates carried Asn, followed by Ser at ~39% and Lys at ~18%. In avian-origin IAVs, the frequency was ~49% for Asn, ~45% for Ser, and ~4.6% for glycine (Gly or G). In canine-origin IAVs, around ~73% of isolates possessed Asn, followed by aspartic acid (Asp or D) at ~24%. In equine-origin IAVs, 99% of isolates carried Asn. Isolates possessing arginine (Arg or R), histidine (His or H), isoleucine (Ile or I), cysteine (Cys or C), methionine (Met or M), glutamine (Gln or Q), or threonine (Thr or T) at residue 145 were found at a frequency below 1%. Alanine (Ala or A), glutamic acid (Glu or E), leucine (Leu or L), phenylalanine (Phe or F), proline (Pro or P), tryptophan (Trp or W), tyrosine (Tyr or Y), and valine (Val or V) were not observed in any of the isolates from analyzed hosts.

To evaluate the impact of substitutions at residue 145, a panel of viruses carrying single substitutions representing each of the 20 amino acids was generated by reverse genetics (RG) (19, 20) (Fig. 1B). Since these viruses were generated in the context of a swine-origin H3N2 IAV (Fig. 1A), 145 N, 145 K, and 145 S are referred to as naturally occurring substitutions, whereas the remaining substitutions are termed alternative or nonnaturally occurring. Substitutions were introduced into the HA of A/turkey/Ohio/313053/2004 (H3N2), which here is referred to as OH/04 wild-type (wt) virus and naturally carries 145 N (Fig. 1C). Of the 19 OH/04 viruses with a single amino acid mutation at amino acid (aa) 145 (OH/04 HA aa 145 single mutant viruses) rescued, next-generation sequencing analysis revealed that 12 substitutions (145 A, 145 C, 145 G, 145 H, 145 K, 145 L, 145 M, 145 P, 145 Q, 145 R, 145 S, and 145 T) were well tolerated (98 to 100% of sequenced reads possessed the expected codon at residue 145) after 3

TABLE 1 Agglutination of erythrocytes by OH/04 aa 145 single mutant viruses

	HA titer (HAU) with:		
Amino acid at position 145	**0.5% turkey RBCs**	**0.5% chicken RBCs**	**1% horse RBCs**
N (wt)	128	256	<2
A	128	64	<2
C	4	<2	<2
F	128	16	8
G	128	32	<2
H	256	128	<2
I	128	64	<2
K	128	128	<2
L	128	128	<2
M	128	128	<2
P	128	64	<2
Q	256	128	<2
R	128	64	<2
S	128	128	<2
T	128	64	<2
V	128	32	<2
Y	128	32	<2

passages in Madin-Darby canine kidney (MDCK) cells. For substitutions 145 F, 145 I, 145 V, and 145 Y, the percentage of reads bearing the mutated codon was around 90% while the remaining 10% of reads showed a partial reversion to the wt codon (I 145 N, V 145 N, and Y 145 N) or a partial transition for a codon specifying Ser (F 145 S). None of these HA substitutions led to compensatory substitutions in the HA or neuraminidase (NA) segments. Three substitutions (145 D, 145 E, and 145 W) were not well tolerated, leading to partial reversion to the wt codon (D 145 N) or partial transition to a codon specifying either Gly (E 145 G) or Leu (W 145 L). Moreover, additional substitutions emerged on the HA for 145 E and 145 W (T 128 A) or on the NA for 145 E (T 148 I). For these reasons, 145 D, 145 E, and 145 W viruses were excluded from further analysis.

Viruses were assayed for their ability to agglutinate red blood cells (RBCs) from different species (turkey, chicken, and horse) by standard hemagglutination (HA) assay. Turkey and chicken RBCs are known to carry both SAα2-3Gal and SAα2-6Gal receptors on their cell surfaces, while horse RBCs display mainly SAα2-3Gal (21–23). Similar to the case for the 145 N (wt) virus, nearly all mutant viruses were found to agglutinate turkey RBCs efficiently, with the exception of 145 C virus, which displayed low HA titers (Table 1). In contrast, agglutination of chicken RBCs was less consistent, with HA titers of some mutant viruses comparable to that of the 145 N (wt) virus and other mutant viruses exhibiting an 8- to 16-fold decrease in HA titers (145 F, 145 G, 145 V, and 145 Y viruses) or no agglutination (145 C virus) (Table 1). Only the 145 F virus showed detectable, albeit low, HA titers using horse RBCs (Table 1). There was no correlation between the ability to agglutinate RBCs and virus titers. Due to the decreased ability to agglutinate RBCs, the 145 C virus was not tested in further assays.

Viruses were then compared in a multiple-step infection cycle *in vitro*. MDCK cells were infected at a low multiplicity of infection (MOI) (0.01). All viruses grew to high titers and displayed similar growth kinetics (Fig. 2A). There was no discernible difference in peak titers ($\sim$6.5 to 7.0 $\log_{10}$ 50% tissue culture infective dose [$TCID_{50}$]/ml equivalents) at 72 h postinfection (hpi), with the exception of the 145 P and 145 H viruses, which showed slightly lower peak titers ($\sim$5.5 $\log_{10}$ $TCID_{50}$/ml equivalents) ($P < 0.001$). Taken together, these results indicate that residue 145 shows high levels of plasticity *in vitro* despite of the limited detection of amino acid variation in nature. Furthermore, single amino acid substitutions did not have a major impact on growth kinetics *in vitro* but modulated the ability of mutant viruses to agglutinate RBCs from particular hosts.

Viruses with alternative substitutions at residue 145 retain SAα2-6Gal binding but frequently display decreased receptor binding avidity. To further expand on

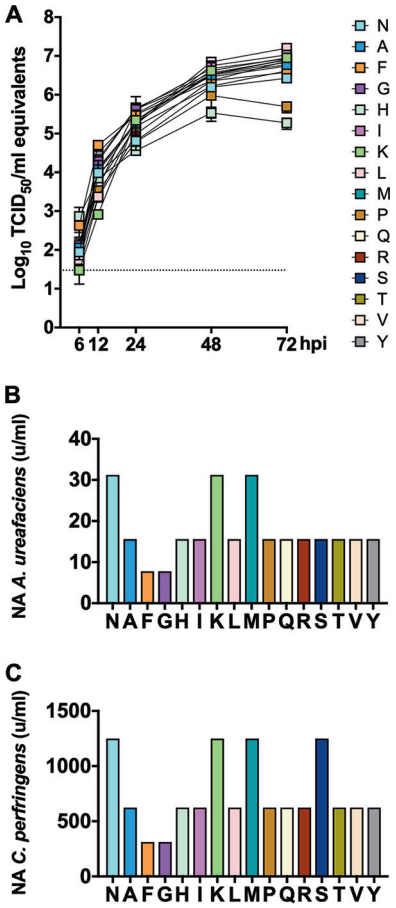

FIG 2 Substitutions at residue 145 show no major impact on virus growth but decrease receptor binding avidity. (A) Confluent monolayers of MDCK cells were inoculated with H3 viruses carrying amino acid substitutions at residue 145 at an MOI of 0.01 and incubated at 37°C. At 6, 12, 24, 48, and 72 hpi, tissue culture supernatants from inoculated cells were collected for virus RNA quantification by rRT-PCR, which was expressed as $\log_{10}$ $TCID_{50}$/ml equivalents. Plotted data represent means ± standard deviations (SD). (B and C) Turkey red blood cells pretreated with different amounts of neuraminidase from either *Clostridium perfringens* (B) or *Arthrobacter ureafaciens* (C) were mixed with H3 viruses carrying amino acid substitutions at residue 145 to quantify virus agglutination as a measure of virus binding avidity. Data are expressed as the maximal amount of neuraminidase that allowed full agglutination. Panels B and C show representative data of one out of two and three independent experiments, respectively, with samples run in duplicates in each experiment. Plotted data represent means ± standard deviations (SD).

the receptor binding characterization of the aa 145 mutants, we analyzed whether these substitutions were involved in modulating receptor avidity or receptor specificity by measuring agglutination of turkey RBCs previously treated with different concentrations of bacterial neuraminidase (Fig. 2B and C). All of the mutant viruses bound to desialylated RBCs to various degrees. Naturally occurring substitutions showed the highest avidity to receptors. Binding of 145 N (wt) virus was indistinguishable from that of either the 145 K (RBC treated with both neuraminidases) or 145 S (RBC treated with *Clostridium perfringens* neuraminidase) virus. Nearly all mutant viruses carrying alternative substitutions at residue 145 displayed decreased receptor binding avidity, with the notable exception of the 145 M virus, which showed no discernible difference in binding compared to the 145 N (wt) virus. Overall, the results suggest differences in avidity regardless of the bacterial neuraminidases tested, although specificity cannot be completely ruled out.

Next, we performed a glycan-based enzyme-linked immunosorbent assay (ELISA) using monospecific preparations of horseradish peroxidase (HRP)-conjugated fetuin (Fet-HRP) as surrogates of binding to SAα2-3Gal (3-Fet-HRP) or SAα2-6Gal (6-Fet-HRP) (24) glycans (Fig. 3A to P). The assay reliably discriminated receptor binding specificity

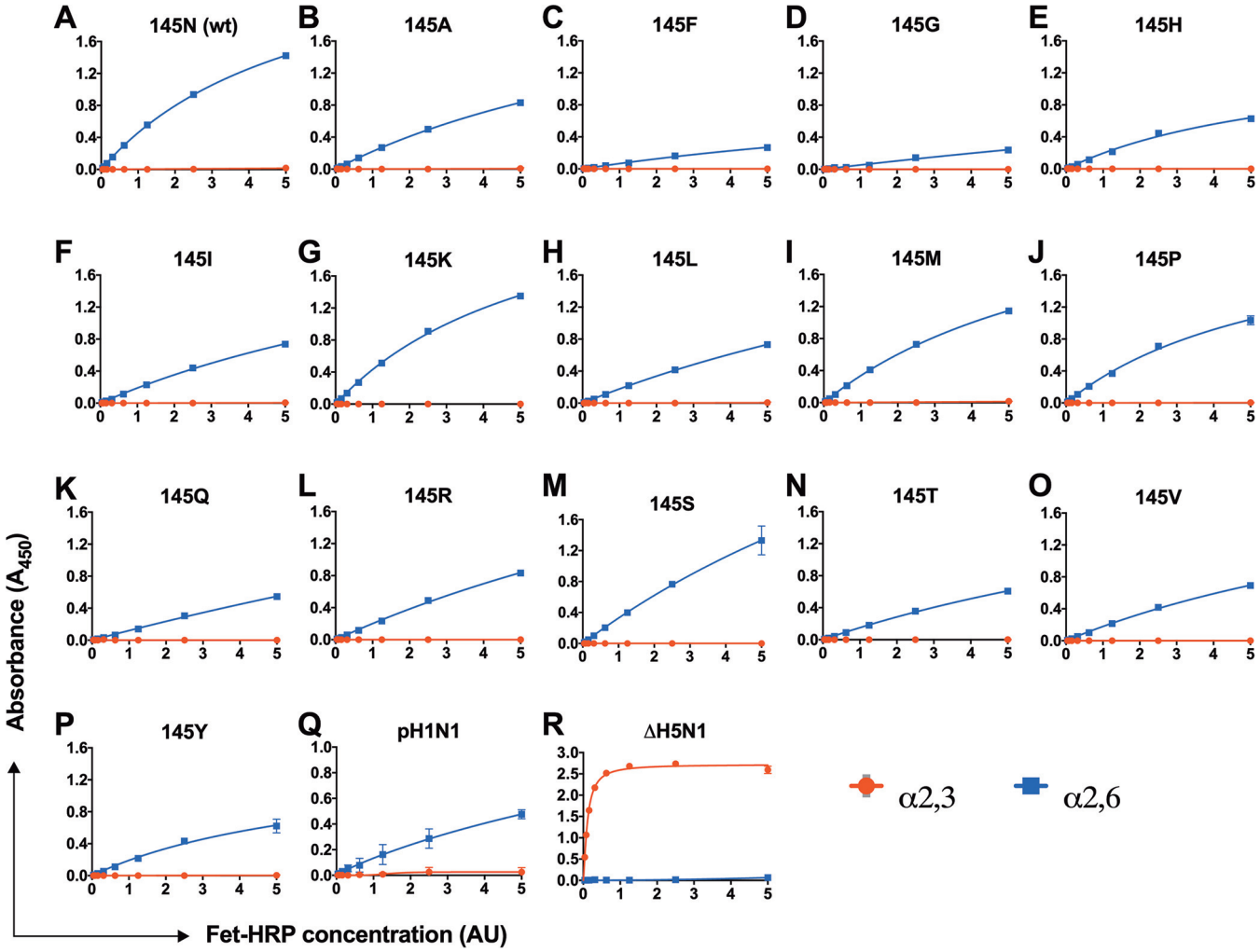

FIG 3 Mutants with substitutions at residue 145 retain binding to SAα2-6Gal. H3 viruses carrying amino acid substitutions at residue 145 were tested for receptor binding specificity with various concentrations of SAα2-3Gal (α-2,3-linked SA) or SAα2-6Gal (α-2,6-linked SA). (A to P) 145 N (wt) virus (A); 145 A virus (B); 145 F virus (C); 145 G virus (D); 145 H virus (E); 145 I virus (F); 145 K virus (G); 145 L virus (H); 145 M virus (I); 145 P virus (J); 145 Q virus (K); 145 R virus (L); 145 S virus (M); 145 T virus (N); 145 V virus (O); 145 Y virus (P). (Q and R) Human pH1N1 (Q) and avian ΔH5N1 (R) were used as controls for binding to SAα2-6Gal and SAα2-3Gal, respectively. Glycan concentration is expressed as arbitrary units (AU). Plotted data represent means ± standard deviations (SD). Data are representative of 2 independent experiments with 2 replicates per experiment.

as evidenced by the viruses used as controls, with human pH1N1 showing a preference to SAα2-6Gal (Fig. 3Q) while avian ΔH5N1 displayed restricted binding to SAα2-3Gal (Fig. 3R). All of the mutant viruses retained binding to SAα2-6Gal with no residual binding to SAα2-3Gal. Naturally occurring substitutions (145 N [wt], 145 K, and 145 S viruses) showed the greatest binding to SAα2-6Gal (Fig. 3A, G, and M). Consistent with differences in avidity from previous results, mutant viruses carrying alternative substitutions at residue 145 displayed weaker binding to SAα2-6Gal (Fig. 3B, F, H to L, and N to P) than viruses possessing naturally occurring substitutions. Among mutant viruses carrying alternative substitutions, 145 M and 145 P viruses demonstrated the highest binding (Fig. 3I and J), while 145 F and 145 G viruses showed substantial decreases in binding to SAα2-6Gal (Fig. 3C and D). Overall, these results suggest that substitutions in HA at residue 145 do not affect receptor specificity but modulate receptor avidity. Nearly all the alternative substitutions led to decreased receptor binding avidity.

Substitutions at residue 145 modulate binding to a broad range of SAα2-6Gal glycans. To further compare the impacts of substitutions at residue 145 on receptor binding specificity, glycan array analysis was performed for all viruses using a glycan microarray containing linear, O-linked, and N-linked glycans with extended poly-*N*-

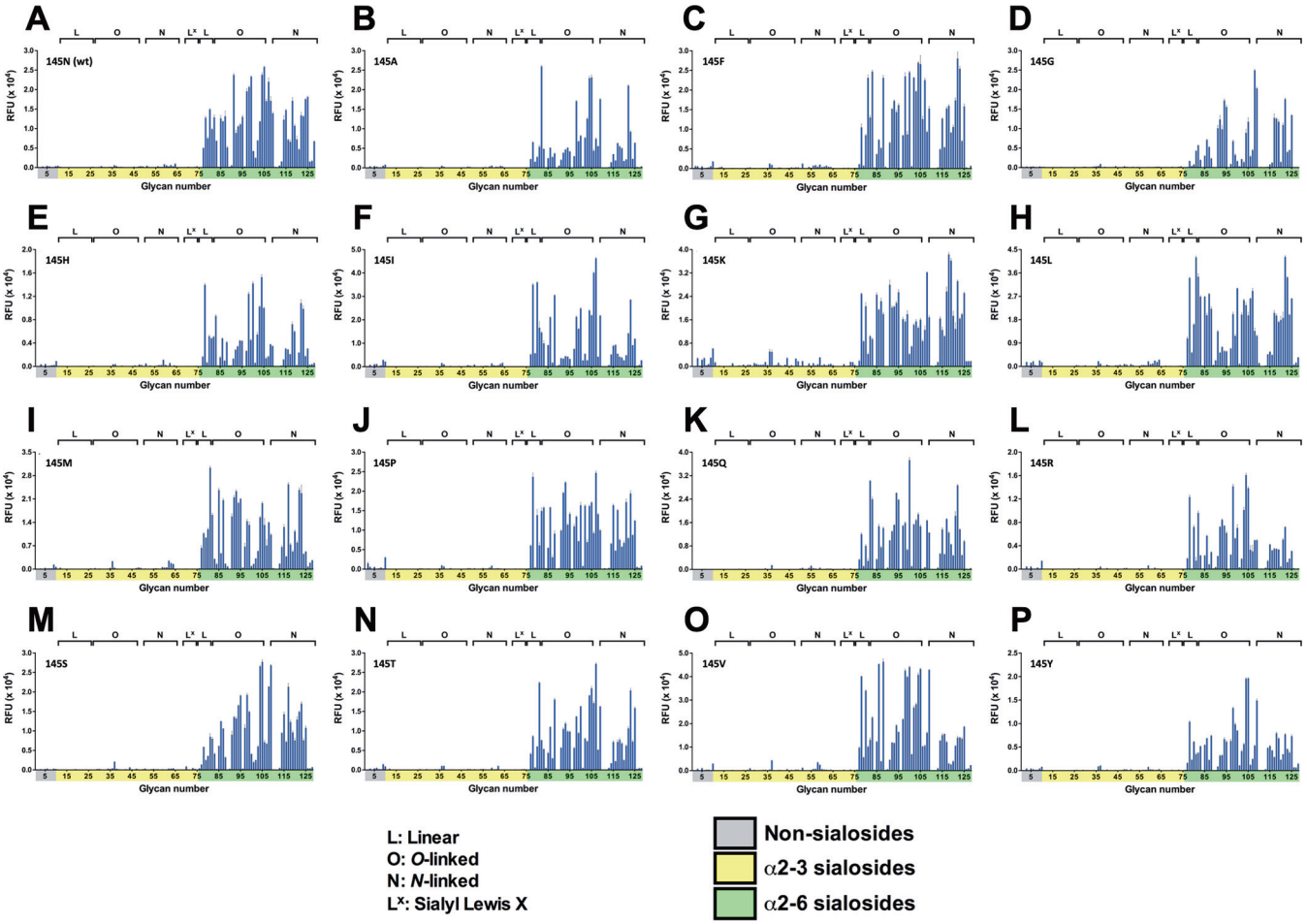

FIG 4 Substitutions at residue 145 modulate binding to a broad range of SAα2-6Gal glycans. Glycan microarray analysis of H3 viruses carrying amino acid substitutions at residue 145 was performed. The array is comprised of nonsialoside control (1 to 10; gray), SAα2-3Gal (11 to 76; yellow), and SAα2-6Gal (77 to 128; green) glycans. Glycans are grouped by structure type: L, linear; O, O linked; N, N linked; and L^x, sialyl Le^x. (A) 145 N (wt) virus; (B) 145 A virus; (C) 145 F virus; (D) 145 G virus; (E) 145 H virus; (F) 145 I virus; (G) 145 K virus; (H) 145 L virus; (I) 145 M virus; (J) 145 P virus; (K) 145 Q virus; (L) 145 R virus; (M) 145 S virus; (N) 145 T virus; (O) 145 V virus; (P) 145 Y virus. Plotted data represent means $\pm$ standard deviations (SD) using four replicates per virus. RFU, relative fluorescence units.

acetyl-lactosamine (poly-LacNAc) repeats found in human, swine, and ferret airway tissues (25). The array provides a broad semiquantitative view of the binding preference for specific viruses. All of the viruses retained specificity to SAα2-6Gal glycans (Fig. 4A to P), corroborating the results from the glycan-based ELISA (Fig. 3). Viruses carrying naturally occurring substitutions showed expanded binding to nearly all SAα2-6Gal glycan types in the array. OH/04 wt (145 N) virus had slightly preferred binding to O-glycans (Fig. 4A), while 145 K virus appeared to favor binding to N-glycans (Fig. 4G). 145 S virus showed a slight reduction in binding to linear and some of the smaller O-glycans (Fig. 4M) compared to OH/04 wt (145 N) virus (Fig. 4A). There were distinct patterns of binding for viruses carrying alternative substitutions. 145 F, 145 L, 145 M, 145 P, 145 Q, 145 T, and 145 V viruses demonstrated binding to a broader range of glycans that was comparable to that for OH/04 wt (145 N) virus (Fig. 4C, H, I, and K to O). The 145 A, 145 G, 145 H, 145 I, 145 R, and 145 Y mutant viruses displayed a more restricted binding to glycans in the array, although they appear to maintain a preference for O-linked glycans (Fig. 4B, D to F, L, and P). Taken together with the glycan-based ELISA results, these data indicated that while certain substitutions in HA at residue 145 lead to broad reductions in binding to SAα2-6Gal glycans, many nonnatural variants appear to be well tolerated, with only minor variance in receptor specificity detected.

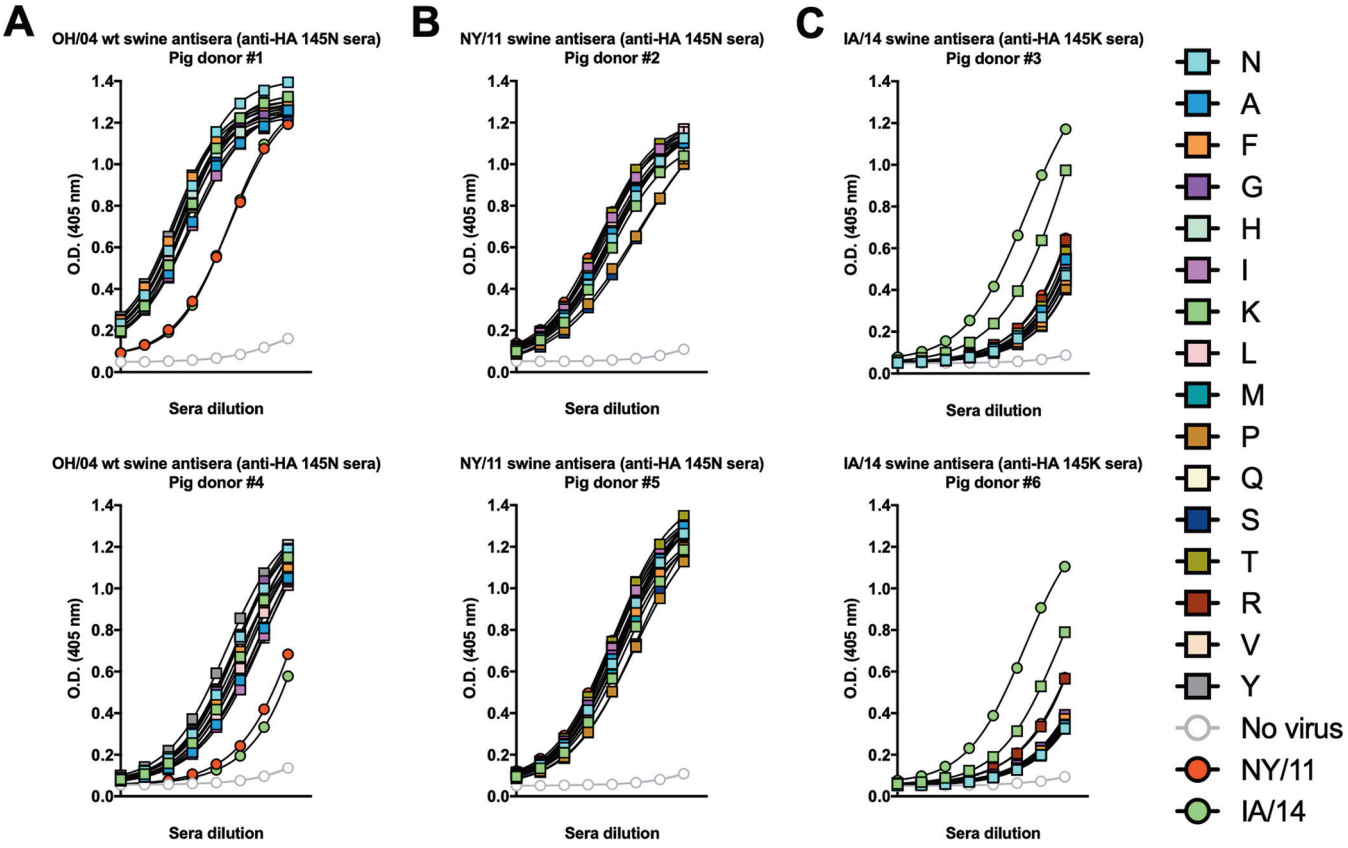

FIG 5 Substitutions at residue 145 modulate serum reactivity. Antibody responses to H3 viruses carrying amino acid substitutions at residue 145 was determined by ELISA using swine antisera generated against OH/04 (A), NY/11 possessing HA residue 145 N (B), or IA/14 possessing HA residue 145 K (C). Two sets of sera were tested independently. The first set of sera was tested 2 times in duplicates. The second set of sera was tested only once in duplicate. Plotted data represent means ± standard deviations (SD). O.D., optical density.

Substitutions at residue 145 modulate serum reactivity. For human H3N2 IAVs, it has been proposed that the emergence of the HA N 145 K substitution led to a change in antibody immunodominance (7). To assess whether a similar phenomenon occurs in swine-origin H3 IAVs and how alternative substitutions at residue 145 affect antigenicity, the serum reactivity of each mutant virus in the panel was tested by ELISA (Fig. 5A to C) and hemagglutination inhibition (HI) assays (Fig. 6A and B). For these experiments, swine antisera against NY/11 or IA/14 wild type viruses were tested. The HA1 domains of these viruses differ by only two amino acids: NY/11 virus possesses 145 N/289 P, while IA/14 carries 145 K/289 S. Based on its location at the base of the HA1 globular head and no prior evidence of an antigenic role, we assume that position 289 is antigenically irrelevant. Additionally, swine antisera against OH/04 wt virus were tested. To prevent confounding effects, the HA gene segments of the NY/11 and IA/14 viruses were rescued by reverse genetics in the background of 7 gene segments from the OH/04 wt virus. The 1 + 7 NY/11 and IA/14 reverse genetics viruses were used as controls in ELISA and HI assays.

The reactivities of sera generated against the OH/04 wt virus were similar across the entire panel of OH/04 aa 145 single mutant viruses (Fig. 5A), indicating that substitutions at residue 145 in the context of OH/04 HA do not change antigenicity against wt homologous sera. Consistent with amino acid divergence between OH/04 wt and control viruses, OH/04 wt virus antisera had reduced reactivity to both NY/11 and IA/14 control viruses. Surprisingly, sera raised against the NY/11 virus displayed no discernible difference in reactivity among all of the viruses evaluated regardless of the aa 145 substitution, including the NY/11 and IA/14 viruses (Fig. 5B). As observed for human H3N2 IAVs, the presence of 145 K in a swine-origin IAV results in an immunodominant

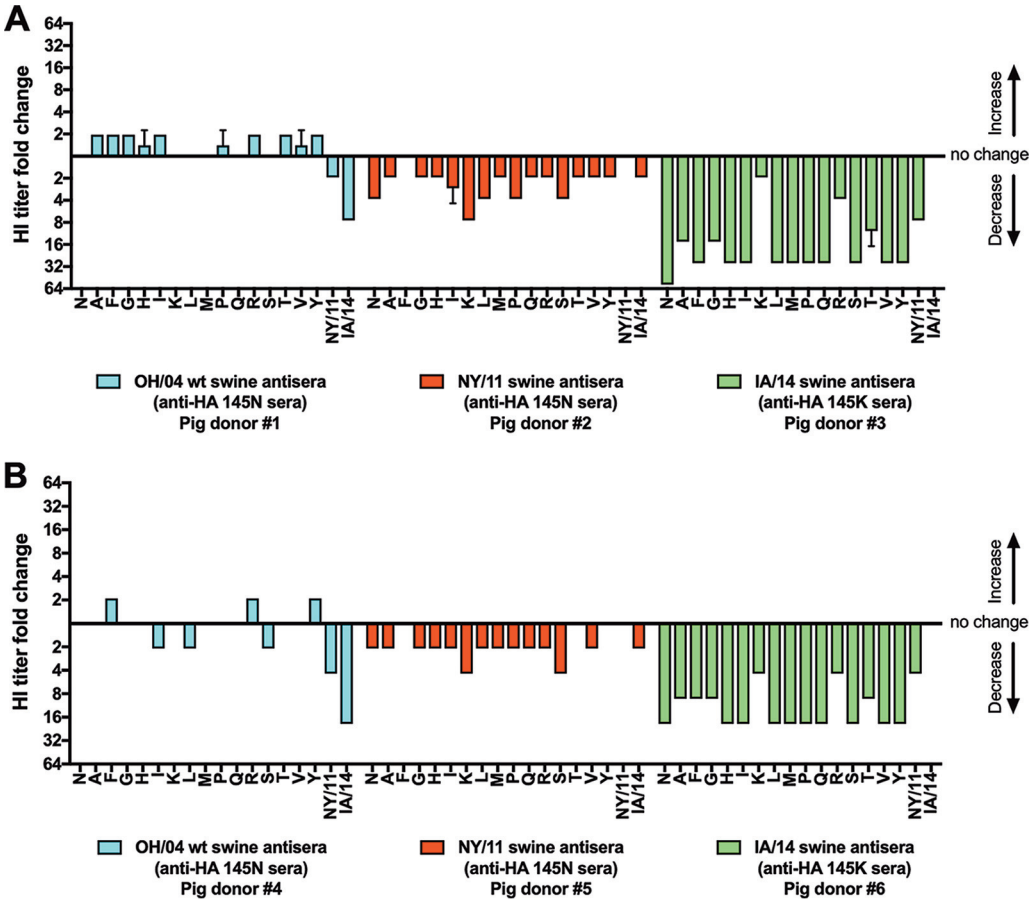

FIG 6 Substitutions at residue 145 impact HI titers. HI titers were measured against H3 viruses carrying amino acid substitutions at residue 145 using swine antisera generated against OH/04 (cyan), NY/11 possessing HA residue 145 N (red) or IA/14 possessing HA residue 145 K (light green). For each panel, two sets of sera were tested independently. The first set of sera was tested 3 times in duplicates. Confirmatory tests were run on a second set of sera, which was tested once in duplicates. The serum reactivities of all H3 mutant viruses to the respective swine antisera are depicted as fold change ($\log_2$ HI titer for mutant virus/$\log_2$ HI titer for homologous virus). Plotted data represent means ± standard deviations (SD). Colors are based on the antigenic cluster designation for swine H3N2 IAVs.

epitope targeted by the antibody response (Fig. 5C). Sera generated against the IA/14 virus showed decreased reactivity to the NY/11 virus (possessing HA residue 145 N) compared to the IA/14 virus (carrying HA residue 145 K). Nearly all of the OH/04 aa 145 single mutant viruses, with the exception of 145 K virus, exhibited diminished reactivity to the IA/14 virus antisera. The 145 K virus was the only mutant virus to consistently show reactivity more similar to that of homologous IA/14 sera generated against the IA/14 virus, confirming the impact of HA residue 145 K in modulating antibody immunodominance.

Antigenic characterization by HI assay was mostly consistent with the ELISA data. The OH/04 wt virus antisera reacted to all OH/04 aa 145 single mutant viruses. Relative to the 145 N (wt) virus, changes in HI titers were almost indistinguishable (Fig. 6A and B). The OH/04 wt virus antisera had a large reduction in cross-HI reactivity against the IA/14 virus and only a modest reduction against the NY/11 virus. Similar to the ELISA data, most substitutions at residue 145 minimally affected NY/11 virus antiserum reactivity, with the 145 K virus causing the largest reduction in cross-HI titers. Reactivity of the IA/14 virus antisera was drastically reduced against nearly all of the OH/04 aa 145 single mutant viruses. In agreement with previous results, the 145 K virus was the only mutant virus to show minimal reduction in serum cross-reactivity compared to IA/14 virus. Collectively, these results indicate that residue 145 K has a profound impact on modulating antibody immunodominance and that serum raised against a 145 K bear-

ing virus can recognize the epitope bearing such a substitution in the context of a distinct H3 HA.

DISCUSSION

HA engagement with terminal SA residues on host cells is an essential step in the IAV replication cycle. Not surprisingly, receptor binding specificity is a major host range restriction factor. In a simplistic view, IAVs of avian origin prefer binding to SAα2-3Gal glycans, whereas those that circulate in humans favor binding to SAα2-6Gal receptors (5, 26–28). During human adaptation of avian-origin IAVs, the receptor specificity switch is accompanied by specific substitutions on the HA (E 190 D/G 225 D in the H1 subtype and Q 226 L/G 228 S in the H2 and H3 subtypes) (5, 26, 29, 30). While these residues are critical to receptor binding specificity, other residues on the HA have the potential to affect receptor binding functions, including receptor binding avidity (7, 8, 23, 31). The identification of up to 7 residues (residues 145, 155, 156, 158, 159, 189, and 193) near the RBS as the major determinants of antigenic drift during the evolution of human and swine H3N2 IAVs (17, 18, 32) has led to the hypothesis that emerging substitutions in these residues must drive antigenic change and immune escape without disrupting receptor binding properties, potentially limiting the flexibility of amino acid residues in these positions (17, 33). In agreement with this hypothesis, analysis of HA sequences showed the occurrence of only a small subset of amino acid substitutions at these residues that are recycled sporadically (17, 18, 32, 34, 35).

Here we examined the amino acid plasticity at residue 145, one of the identified key determinants of antigenic drift, by mutating this residue to create a panel of H3 HA mutant viruses carrying a single amino acid substitution, representing every possible amino acid in a swine H3N2 backbone. HA residue 145 showed extraordinary plasticity, with 16 out of 19 substitutions (145 A, 145 C, 145 F, 145 G, 145 H, 145 I, 145 K, 145 L, 145 M, 145 P, 145 Q, 145 R, 145 S, 145 T, 145 V, and 145 Y) being well tolerated *in vitro* (with 90 to 100% of sequenced reads possessing the mutated codon at residue 145). Whether these substitutions are tolerated *in vivo* is beyond the scope of the present report and remain to be determined. Consistent with the intricate balance between immune escape and receptor binding, three substitutions (145 D, 145 E, and 145 W) were not tolerated and led to the emergence of partial reversion at residue 145 and additional substitutions in HA (T 128 A) and/or NA (T 148 I). HA T 128 A disrupted a potential glycosylation site (36, 37) and was shown to emerge along with a substitution at residue 145 in human H3N2 IAVs during the 2013 to 2014 season (34). NA T 148 I has been associated with reduced NA activity, decreased susceptibility to neuraminidase inhibitors, and NA-mediated binding and agglutination (38, 39). The previously reported role of these substitutions suggests that they may be compensatory.

With the exception of 145 C virus, there was no discernible difference in the abilities of the tested mutant viruses to agglutinate turkey RBCs. Turkey and chicken RBCs carry both SAα2-3Gal and SAα2-6Gal glycans on their cell surface (21–23), and some of tested mutant viruses exhibited an impaired ability to agglutinate chicken RBCs. Loss of the ability to agglutinate RBCs has plagued the antigenic characterization of recent human H3N2 IAVs (40). As previously reported for chicken RBCs (41), an in-depth analysis of major glycan structures present on RBCs from other hosts will help shed light on current issues on antigenic characterization of IAVs.

Using independent assays, we demonstrated that all tested mutant viruses retained some binding to SAα2-6Gal glycans. However, viruses possessing naturally occurring substitutions (145 N [wt], 145 K, and 145 S) showed the strongest receptor binding. With the exception of 145 M virus, all viruses carrying alternative substitutions (145 A, 145 C, 145 F, 145 G, 145 H, 145 I, 145 L, 145 P, 145 Q, 145 R, 145 T, 145 V, and 145 Y) displayed a decreased ability to bind SAα2-6Gal receptors. In contrast to other reports, no compensatory substitutions were identified on the HA or NA by next-generation sequencing (42, 43). This indicates that the observed changes in receptor binding reported here are directly related to substitutions at residue 145. It is important to emphasize that although viruses carrying alternative substitutions exhibited decreased

receptor binding avidity *in vitro*, the lower threshold for biologically relevant avidity *in vivo* is unknown. Glycan array analysis revealed a broad range of SAα2-6Gal glycan interactions that were modulated by substitutions at residue 145. Interestingly, one of the viruses with the lowest binding to 6-modified fetuin glycans in the panel (145 F virus) displayed extensive binding to SAα2-6Gal glycans, including extended glycans (25). While the expanded glycan array provides important insights on the binding preference, the question of which receptors are relevant for IAV attachment and transmission *in vivo* remains to be elucidated. Furthermore, the density, distribution, and organization of glycans on host tissues are poorly defined.

As observed in human H3N2 IAVs, the emergence of the HA N 145 K substitution in swine H3N2 IAVs led to a change in the antibody immunodominance. It is astonishing that reactivity to sera raised against a virus possessing HA 145 N was indistinguishable among all of the viruses carrying substitutions at residue 145, but reactivity to sera raised against a virus possessing HA 145 K was highly skewed to recognize an epitope bearing HA residue 145 K even in the context of a distantly related H3 HA, demonstrating the dramatic impact that N 145 K mutants can have on population immunity. Antibody immunodominance may be key for understanding antigenic drift and refers to the immunological phenomenon in which the immune system preferentially mounts a response to complex antigens in a dynamic hierarchical order (14). Immunodominance hierarchy can occur at the level of viruses within multivalent immunogens, proteins within viruses, antigenic sites within proteins, epitopes within antigenic sites, and, as shown in the present report and by others, single amino acid substitutions within epitopes (7, 14, 16, 17, 44, 45). The impact of substitutions at residue 145 on immunogenicity and antibody immunodominance remains to be fully characterized. While there may be a fitness cost associated with the emergence of such substitutions in nature, the ability to manipulate the amino acid plasticity near the RBS may offer an alternative approach to induce broader protection and, perhaps, potentially elicit receptor mimicry and broad-spectrum neutralizing antibodies (46).

The complex and continuous antigenic evolution of IAVs remains a major hurdle for vaccine selection and effective vaccination. We provide a better understanding of the functional effects of amino acid substitutions near the RBS that are implicated in antigenic drift and their consequences for receptor binding. The mutation analyses presented in this report represent a significant data set to aid and test the ability of computational approaches to predict binding of glycans.

MATERIALS AND METHODS

Cell culture. Madin-Darby canine kidney (MDCK) and human embryonic kidney 293T cells were maintained in Dulbecco's modified Eagle's medium (DMEM) supplemented with 10% fetal bovine serum (FBS). Cells were propagated at 37°C in a humidified incubator under a 5% CO_2 atmosphere.

Molecular cloning and virus rescue. The OH/04 wt strain is a prototypic swine-origin virus amenable to genetic manipulation by an established reverse genetics (RG) system (18, 47, 48). Single amino acid substitutions representing each of the 20 naturally occurring amino acids (Table 2) were inserted by site-directed mutagenesis at the codon corresponding to HA residue 145 (H3 numbering). To prevent the carryover of OH/04 wt HA plasmid DNA during PCR amplification, the cloned OH/04 wt HA segment was split into two overlapping plasmids, pDP-SD1 and pDP-SD2. The pDP-SD1 plasmid carries the mouse RNA polymerase I terminator (t1) (20) followed by nucleotides 1 to 522 of the OH/04 wt HA segment. The pDP-SD2 plasmid contains nucleotides 500 to 1762 of the OH/04 wt HA segment followed by the human RNA polymerase I promoter (polI) (20). To introduce the desired mutations into OH/04 wt HA, a PCR fragment containing t1 followed by the 5′ portion of the HA was generated with forward primer 5′-ACC GGA GTA CTG GTC GAC CTC CGA AGT TGG GGG GGA GCA AAA GCA GG-3′ and the respective reverse primer (Table 2) using pDP-SD1 as the template. Similarly, a PCR fragment comprising the 3′ portion of HA followed by polI was amplified from pDP-SD2 using reverse primer 5′-ATG CTG ACA ACG TCC CCG GCC CGG CGC TGC T-3′ and the respective forward primer (Table 2). All PCR products were purified by gel extraction using the QIAquick gel extraction kit (Qiagen, Valencia, CA) and combined to produce RG-ready PCR-based HA segments for individual OH/04 HA aa 145 single mutants by overlapping PCR as previously described (19). All PCRs were performed with Phusion high-fidelity DNA polymerase (New England Biolabs, Ipswich, MA), and products were confirmed to be free of unwanted mutations by sequencing. Viruses were rescued by PCR-based RG using a coculture of 293T and MDCK cells as previously described (19, 20). To generate OH/04 HA aa 145 single mutant viruses, the respective RG PCR-based HA segment was paired with the seven plasmids representing the remaining OH/04 wt gene segments. Following transfection, cells were incubated at 35°C. After 24 h of incubation, medium was

TABLE 2 Primers used to introduce amino acid substitutions at residue 145

Amino acid at position 145	Forward primer sequence (5′→3′)[a]	Reverse primer sequence (5′→3′)
A	GGAATCTGTT**GCT**AGTTTCTTTAGTAGATT	TAAAGAAACT**AGC**AACAGATTCCCTTCT
C	GGAATCTGTT**TGT**AGTTTCTTTAGTAGATT	TAAAGAAACT**ACA**AACAGATTCCCTTCT
D	GGAATCTGTT**GAT**AGTTTCTTTAGTAGATT	TAAAGAAACT**ATC**AACAGATTCCCTTCT
E	GGAATCTGTT**GAA**AGTTTCTTTAGTAGATT	TAAAGAAACT**TTC**AACAGATTCCCTTCT
F	GGAATCTGTT**TTT**AGTTTCTTTAGTAGATT	TAAAGAAACT**AAA**AACAGATTCCCTTCT
G	GGAATCTGTT**GGA**AGTTTCTTTAGTAGATT	TAAAGAAACT**TCC**AACAGATTCCCTTCT
H	GGAATCTGTT**CAT**AGTTTCTTTAGTAGATT	TAAAGAAACT**ATG**AACAGATTCCCTTCT
I	GGAATCTGTT**ATA**AGTTTCTTTAGTAGATT	TAAAGAAACT**TAT**AACAGATTCCCTTCT
K	GGAATCTGTT**AAA**AGTTTCTTTAGTAGATT	TAAAGAAACT**TTT**AACAGATTCCCTTCT
L	GGAATCTGTT**CTC**AGTTTCTTTAGTAGATT	TAAAGAAACT**GAG**AACAGATTCCCTTCT
M	GGAATCTGTT**ATG**AGTTTCTTTAGTAGATT	TAAAGAAACT**CAT**AACAGATTCCCTTCT
P	GGAATCTGTT**CCA**AGTTTCTTTAGTAGATT	TAAAGAAACT**TGG**AACAGATTCCCTTCT
Q	GGAATCTGTT**CAA**AGTTTCTTTAGTAGATT	TAAAGAAACT**TTG**AACAGATTCCCTTCT
R	GGAATCTGTT**CGG**AGTTTCTTTAGTAGATT	TAAAGAAACT**CCG**AACAGATTCCCTTCT
S	GGAATCTGTT**AGC**AGTTTCTTTAGTAGATT	TAAAGAAACT**GCT**AACAGATTCCCTTCT
T	GGAATCTGTT**ACA**AGTTTCTTTAGTAGATT	TAAAGAAACT**TGT**AACAGATTCCCTTCT
V	GGAATCTGTT**GTC**AGTTTCTTTAGTAGATT	TAAAGAAACT**GAC**AACAGATTCCCTTCT
W	GGAATCTGTT**TGG**AGTTTCTTTAGTAGATT	TAAAGAAACT**CCA**AACAGATTCCCTTCT
Y	GGAATCTGTT**TAT**AGTTTCTTTAGTAGATT	TAAAGAAACT**ATA**AACAGATTCCCTTCT

[a]Bold nucleotides indicate the mutated codon associated with HA residue 145.

replaced with Opti-MEM I (Life Technologies, Carlsbad, CA) containing 1 μg/ml TPCK (tosylsulfonyl phenylalanyl chloromethyl ketone)-trypsin (Worthington Biochemicals, Lakewood, NJ) and 1% antibiotic-antimycotic solution (Sigma-Aldrich, St. Louis, MO). Following virus rescue, virus stocks were amplified in MDCK cells. Virus stocks were titrated by $TCID_{50}$, and virus titers were determined by the method of Reed and Muench (49).

Whole-genome sequencing. Virus RNA from tissue culture supernatant virus stocks was purified using the RNeasy minikit (Qiagen, Valencia, CA) or the MagNA Pure LC RNA isolation kit (Roche Life Science, Mannheim, Germany). Isolated virus RNA served as the template in a one-step reverse transcriptase PCR (RT-PCR) for multisegment, whole-genome amplification (50). Amplicon sequence libraries were prepared as previously described (50) or using the Nextera XT DNA Library Prep kit (Illumina, San Diego, CA) according to the manufacturer's protocol. Barcoded libraries were multiplexed and sequenced on the high-throughput Illumina MiSeq sequencing platform in a paired-end 150-nucleotide (nt) run format. De novo genome assembly was performed as described previously (50), and HA- and NA-specific reads were mapped to OH/04 reference sequences using Geneious 10.1.3 (51).

***In vitro* growth kinetics.** Confluent monolayers of MDCK cells were inoculated at a multiplicity of infection (MOI) of 0.01 for each virus. After 1 h of incubation, the virus inoculum was removed and cells washed twice with 1× phosphate-buffered saline (PBS). Opti-MEM I (Life Technologies, Carlsbad, CA) containing TPCK-trypsin (Worthington Biochemicals, Lakewood, NJ) and an antibiotic-antimycotic solution (Sigma-Aldrich, St. Louis, MO) was then added to the cells. At the indicated time points, tissue culture supernatant from inoculated cells was collected for virus titer quantification. Virus RNA from tissue culture supernatant was isolated using the MagMAX-96 AI/ND viral RNA isolation kit (Thermo Fisher Scientific, Waltham, MA). Virus titers were determined using a real-time reverse transcriptase PCR (rRT-PCR) assay based on the influenza A matrix gene (52). The rRT-PCR was performed in a LightCycler 480 real-time PCR instrument (Roche Diagnostics, Rotkreuz, Switzerland) using the LightCycler 480 RNA master hydrolysis probe kit (Roche Life Science, Mannheim, Germany). A standard curve was generated using 10-fold serial dilutions from an OH/04 wt virus stock of known titer to correlate quantitative PCR (qPCR) crossing-point (Cp) values with virus titers, as previously described (53). Virus titers were expressed as $\log_{10}$ $TCID_{50}$/ml equivalents.

HA assay. Chicken (Poultry Diagnostic and Research Center, Athens, GA), turkey (Poultry Diagnostic and Research Center, Athens, GA), and horse (Lampire Biologicals, Pipersville, PA) red blood cells (RBCs) were prepared from whole blood preparations using standard techniques (54). Virus HA assays were carried out using 0.5% (vol/vol in PBS) chicken RBCs, 0.5% (vol/vol in PBS) turkey RBCs, or 1% (vol/vol in PBS) horse RBCs. Briefly, 50 μl of RBC preparations was added to 50 μl of 2-fold serial dilutions of virus stocks and allowed to incubate at room temperature for 45 min. After incubation, agglutination was measured, and data were expressed as the inverse of the highest dilution that allowed full agglutination.

Receptor cell binding assay. The receptor cell binding assay was performed as previously described (8, 18, 55). Briefly, 10% (vol/vol in PBS) turkey RBCs were pretreated for 1 h at 37°C with 2-fold serial dilutions of bacterial neuraminidase from *Arthrobacter ureafaciens* (New England BioLabs, Ipswich, MA) or *Clostridium perfringens* (New England BioLabs, Ipswich, MA). Following neuraminidase treatment, treated RBCs were washed twice with cold PBS and then resuspended to 1% (vol/vol in PBS), and then 50 μl of 1% RBCs treated with the different neuraminidase concentrations was added to 50 μl of each virus (8 HA units [HAU], as determined on untreated RBCs) and allowed to incubate at room temperature for 45 min. After incubation, agglutination was measured, and data were expressed as the maximal concentration of neuraminidase that allowed full agglutination.

Solid-phase assay of receptor binding specificity. The receptor-binding specificity was determined in a solid-phase direct binding assay using monospecific preparations of horseradish peroxidase (HRP)-

conjugated fetuin (Fet-HRP). Monospecific preparations of Fet-HRP were synthesized using α-2,3-sialyltransferase from *Pasteurella multocida* (Sigma, St. Louis, MO) for 3-modified fetuin (3-Fet-HRP) or α-2,6-sialyltransferase from *Photobacterium damsela* (Sigma, St. Louis, MO) for 6-modified fetuin (6-Fet-HRP), essentially as described previously (24). Ninety-six-well native fetuin-coated flat-bottom plates (Greiner Bio-One, Monroe, NC) were incubated overnight at 4°C with 128 HAU of each virus in 0.02 M Tris-buffered saline (TBS), pH 7.2 to 7.4. Virus samples were run in duplicate. Plates were washed three times with PBS and blocked with blocking solution (BS) (PBS containing 0.1% neuraminidase-treated bovine serum albumin [BSA-NA]) for 2 h at room temperature. After blocking, plates were washed twice with ice-cold washing solution (WS) (PBS containing 0.02% Tween 80) and incubated with 2-fold serial dilution of 3-Fet-HRP (SAα2-3Gal) or 6-Fet-HRP (SAα2-6Gal) in reaction solution (RS) (PBS containing 0.02% Tween 80, 0.1% BSA-NA, and 2 μM oseltamivir carboxylate) for 1 h at 4°C. After incubation, plates were washed five times with ice-cold WS before adding freshly prepared substrate solution (SS) (0.01% 3,3′,5,5′-tetramethylbenzidine in 0.05 M sodium acetate with 0.03% H_2O_2). Reactions were allowed to proceed at room temperature for 30 min unless otherwise stated. Reactions were stopped with 3% (vol/vol in double-distilled water [ddH_2O]) H_2SO_4. Absorbance readings were obtained at 450 nm using a Victor ×3 multilabel plate reader (PerkinElmer, Waltham, MA).

Glycan array analysis. Virus stocks were grown in MDCK cells, clarified by low-speed centrifugation, and inactivated by treatment with 0.1% β-propiolactone (BPL) for 1 day at 4°C. Inactivated virus stocks were concentrated as described previously (56). Concentrated virus stocks were resuspended in PBS with 5% glycerol to 1280 to 5120 HAU, aliquoted, and stored at −80°C. HA titers of concentrated virus stocks were determined by HA assay using 0.5% (vol/vol in PBS) turkey RBCs. Glycan array analysis was performed using an *N*-hydroxysuccinimide (NHS) ester-coated glass microarray slide containing six replicates of 128 diverse synthetic sialic acid-containing glycans, including terminal sequences as well as N-linked and O-linked glycans found on mammalian and avian glycoproteins and glycolipids (25). Whole influenza virus samples were diluted to 256 HAU in PBS containing 3% BSA (PBS-BSA) and incubated on the array surface for 1 h at room temperature in a humidity-controlled chamber. After incubation, slides were washed in PBS and incubated with OH/04 wt swine antiserum (18) diluted 1:200 in PBS-BSA for 1 h. Slides were washed in PBS and incubated for 1 h in goat anti-pig IgG conjugated to fluorescein isothiocyanate (FITC) (Thermo Fisher Scientific, Waltham, MA) diluted in PBS-BSA (20 μg/ml, final concentration). Slides were washed twice in PBS and in distilled water (dH_2O) and then dried prior to detection. Slide scanning to detect bound virus was conducted using an InnoScan 1100AL (Innopsys, Carbonne, France) fluorescent microarray scanner. Fluorescent signal intensity was measured using Mapix (Innopsys, Carbonne, France), and the mean intensity minus mean background of 4 replicate spots was calculated. A complete list of the glycans present in the array is presented in Table S1 in the supplemental material. The array is comprised of nonsialoside control (1 to 10; gray), SAα2-3Gal (11 to 76; yellow), and SAα2-6Gal (77 to 128; green) glycans. Glycans are grouped by structure type: L, linear; O, O linked; N, N linked; and L^x, sialyl Le^x.

Antisera. Swine antisera against A/swine/New York/A01104005/2011 (H3N2) (NY/11), A/swine/Iowa/A01480656/2014 (H3N2) (IA/14), and A/turkey/Ohio/313053/2004 (H3N2) (OH/04) were generated in previous studies (18, 32). For each virus, two pigs were primed and boosted intramuscularly with UV-inactivated whole-virus vaccine prepared with commercial oil-in-water adjuvant (1:5 ratio) (Emulsigen D; MVP Laboratories, Inc., Ralston, NE). The pigs were humanely euthanized for blood collection.

HI assay. Hemagglutination inhibition (HI) assays were performed as previously described (54). Prior to HI testing, swine antisera were treated overnight with receptor-destroying enzyme (Denka Seiken, Tokyo, Japan) and heat inactivated at 56°C for 30 min. Serial 2-fold dilutions starting at 1:10 were tested for the ability to inhibit the agglutination of 0.5% turkey RBCs with 4 HAU of each virus. HI titers were recorded as the inverse of the highest dilution that inhibited hemagglutination.

ELISA. For enzyme-linked immunosorbent assay (ELISA), 96-well flat-bottom plates (Greiner Bio-One, Monroe, NC) were incubated overnight at 4°C with 16 HAU of each virus in 1× coating solution (Seracare, Milford, MA). Virus samples were run in duplicate. Plates were blocked with StartingBlock (PBS) blocking buffer (Thermo Fisher Scientific, Waltham, MA) for 1 h at room temperature. After blocking, plates were washed three times with PBS containing 0.05% Tween 20 (PBS-T). Twofold serial dilutions of swine antisera were added and allowed to incubate for 1 h at room temperature. After incubation, plates were washed three times with PBS-T before adding the secondary goat anti-swine IgG-HRP HRP-conjugated polyclonal antibody (Seracare, Milford, MA). Plates were incubated at room temperature for 1 h. After incubation, plates were washed three times with PBS-T before treatment with freshly prepared SS buffer or 2, 2′-azino-di(3-ethylbenzthiazoline-6-sulfonate) (ABTS) 1-component microwell peroxidase substrate (Seracare, Milford, MA) for 1 h at room temperature. The reaction was stopped by adding 3% (vol/vol in ddH_2O) H_2SO_4 or ABTS peroxidase stop solution (Seracare, Milford, MA), respectively. Absorbance readings were obtained at 405 nm using a Victor ×3 multilabel plate reader (PerkinElmer, Waltham, MA).

Statistical analysis. All statistical analyses were performed using the GraphPad Prism software, version 7 (GraphPad Software Inc., San Diego, CA). For multiple comparisons, one-way or two-way analysis of variance (ANOVA) followed by a *post hoc* Tukey test was performed. When indicated, a *P* value below 0.05 ($P < 0.05$) was considered significant.

Structure modeling. A model of the structure of the HA of A/turkey/Ohio/313053/2004 (H3N2) was built by homology modeling using Modeller v9.16 (57) based upon the crystal structures of multiple H3 HA proteins (Protein Data Bank [PDB] codes 2YP7, 1HA0, 2YP2, 4WE8, and 4WE5). The generated model was subsequently rendered with PyMOL v2.1 (58).

Computational analysis of HA sequences. The frequency distribution of amino acid identities at residue 145 (H3 numbering) was computed using the sequence variation analysis tool in the Influenza

Research Database (IRD) (59). HA amino acid sequences from IAVs of the H3 subtype isolated from swine, human, avian, canine, and equine hosts and publicly available in the IRD as of 6 September 2017 were analyzed. For humans, the frequency was calculated from precomputed data in the IRD database. Only amino acids that reached a frequency of at least 1% are labeled in the plot legend.

SUPPLEMENTAL MATERIAL

Supplemental material for this article may be found at https://doi.org/10.1128/JVI.01413-18.

SUPPLEMENTAL FILE 1, PDF file, 4.1 MB.

ACKNOWLEDGMENTS

This study was supported by a subcontract from the Center for Research on Influenza Pathogenesis (CRIP) to D.R.P. under contract HHSN272201400008C from the National Institute of Allergy and Infectious Diseases (NIAID) Centers for Influenza Research and Surveillance (CEIRS) and by NIH grant AI114730 to J.C.P. J.J.S.S. received a short-term training award from the NIAID CEIRS Training Program, HHSN272201400008C. Additional funding was supplied by the Kwang Hua Educational Foundation to J.C.P. This study was also supported in part by resources and technical expertise from the Georgia Advanced Computing Resource Center, a partnership between the University of Georgia's Office of the Vice President for Research and Office of the Vice President for Information Technology.

REFERENCES

1. Nicholls JM, Chan RW, Russell RJ, Air GM, Peiris JS. 2008. Evolving complexities of influenza virus and its receptors. Trends Microbiol 16:149–157. https://doi.org/10.1016/j.tim.2008.01.008.
2. Wilson IA, Skehel JJ, Wiley DC. 1981. Structure of the haemagglutinin membrane glycoprotein of influenza virus at 3 A resolution. Nature 289:366–373. https://doi.org/10.1038/289366a0.
3. Skehel JJ, Wiley DC. 2000. Receptor binding and membrane fusion in virus entry: the influenza hemagglutinin. Annu Rev Biochem 69:531–569. https://doi.org/10.1146/annurev.biochem.69.1.531.
4. Matrosovich M, Tuzikov A, Bovin N, Gambaryan A, Klimov A, Castrucci MR, Donatelli I, Kawaoka Y. 2000. Early alterations of the receptor-binding properties of H1, H2, and H3 avian influenza virus hemagglutinins after their introduction into mammals. J Virol 74:8502–8512. https://doi.org/10.1128/JVI.74.18.8502-8512.2000.
5. Connor RJ, Kawaoka Y, Webster RG, Paulson JC. 1994. Receptor specificity in human, avian, and equine H2 and H3 influenza virus isolates. Virology 205:17–23. https://doi.org/10.1006/viro.1994.1615.
6. Wan H, Perez DR. 2007. Amino acid 226 in the hemagglutinin of H9N2 influenza viruses determines cell tropism and replication in human airway epithelial cells. J Virol 81:5181–5191. https://doi.org/10.1128/JVI.02827-06.
7. Li Y, Bostick DL, Sullivan CB, Myers JL, Griesemer SB, Stgeorge K, Plotkin JB, Hensley SE. 2013. Single hemagglutinin mutations that alter both antigenicity and receptor binding avidity influence influenza virus antigenic clustering. J Virol 87:9904–9910. https://doi.org/10.1128/JVI.01023-13.
8. Hensley SE, Das SR, Bailey AL, Schmidt LM, Hickman HD, Jayaraman A, Viswanathan K, Raman R, Sasisekharan R, Bennink JR, Yewdell JW. 2009. Hemagglutinin receptor binding avidity drives influenza A virus antigenic drift. Science 326:734–736. https://doi.org/10.1126/science.1178258.
9. Nelson MI, Vincent AL. 2015. Reverse zoonosis of influenza to swine: new perspectives on the human-animal interface. Trends Microbiol 23:142–153. https://doi.org/10.1016/j.tim.2014.12.002.
10. Belongia EA, Simpson MD, King JP, Sundaram ME, Kelley NS, Osterholm MT, McLean HQ. 2016. Variable influenza vaccine effectiveness by subtype: a systematic review and meta-analysis of test-negative design studies. Lancet Infect Dis 16:942–951. https://doi.org/10.1016/S1473-3099(16)00129-8.
11. Rajao DS, Perez DR. 2018. Universal vaccines and vaccine platforms to protect against influenza viruses in humans And Agriculture. Front Microbiol 9:123. https://doi.org/10.3389/fmicb.2018.00123.
12. Altman MO, Bennink JR, Yewdell JW, Herrin BR. 2015. Lamprey VLRB response to influenza virus supports universal rules of immunogenicity and antigenicity. Elife 4. https://doi.org/10.7554/eLife.07467.
13. Virelizier JL. 1975. Host defenses against influenza virus: the role of anti-hemagglutinin antibody. J Immunol 115:434–439.
14. Altman MO, Angeletti D, Yewdell JW. 2018. Antibody immunodominance: the key to understanding influenza virus antigenic drift. Viral Immunol 31:142–149. https://doi.org/10.1089/vim.2017.0129.
15. Chambers BS, Parkhouse K, Ross TM, Alby K, Hensley SE. 2015. Identification of hemagglutinin residues responsible for H3N2 antigenic drift during the 2014-2015 influenza season. Cell Rep 12:1–6. https://doi.org/10.1016/j.celrep.2015.06.005.
16. Smith DJ, Lapedes AS, de Jong JC, Bestebroer TM, Rimmelzwaan GF, Osterhaus AD, Fouchier RA. 2004. Mapping the antigenic and genetic evolution of influenza virus. Science 305:371–376. https://doi.org/10.1126/science.1097211.
17. Koel BF, Burke DF, Bestebroer TM, van der Vliet S, Zondag GC, Vervaet G, Skepner E, Lewis NS, Spronken MI, Russell CA, Eropkin MY, Hurt AC, Barr IG, de Jong JC, Rimmelzwaan GF, Osterhaus AD, Fouchier RA, Smith DJ. 2013. Substitutions near the receptor binding site determine major antigenic change during influenza virus evolution. Science 342:976–979. https://doi.org/10.1126/science.1244730.
18. Abente EJ, Santos J, Lewis NS, Gauger PC, Stratton J, Skepner E, Anderson TK, Rajao DS, Perez DR, Vincent AL. 2016. The molecular determinants of antibody recognition and antigenic drift in the H3 hemagglutinin of swine influenza A virus. J Virol 90:8266–8280. https://doi.org/10.1128/JVI.01002-16.
19. Chen H, Ye J, Xu K, Angel M, Shao H, Ferrero A, Sutton T, Perez DR. 2012. Partial and full PCR-based reverse genetics strategy for influenza viruses. PLoS One 7:e46378. https://doi.org/10.1371/journal.pone.0046378.
20. Perez DR, Angel M, Gonzalez-Reiche AS, Santos J, Obadan A, Martinez-Sobrido L. 2017. Plasmid-based reverse genetics of influenza A virus. Methods Mol Biol 1602:251–273. https://doi.org/10.1007/978-1-4939-6964-7_16.
21. Ito T, Suzuki Y, Mitnaul L, Vines A, Kida H, Kawaoka Y. 1997. Receptor specificity of influenza A viruses correlates with the agglutination of erythrocytes from different animal species. Virology 227:493–499. https://doi.org/10.1006/viro.1996.8323.
22. Medeiros R, Escriou N, Naffakh N, Manuguerra JC, van der Werf S. 2001. Hemagglutinin residues of recent human A(H3N2) influenza viruses that contribute to the inability to agglutinate chicken erythrocytes. Virology 289:74–85. https://doi.org/10.1006/viro.2001.1121.
23. Bradley KC, Galloway SE, Lasanajak Y, Song X, Heimburg-Molinaro J, Yu H, Chen X, Talekar GR, Smith DF, Cummings RD, Steinhauer DA. 2011. Analysis of influenza virus hemagglutinin receptor binding mutants with

limited receptor recognition properties and conditional replication characteristics. J Virol 85:12387–12398. https://doi.org/10.1128/JVI.05570-11.
24. Matrosovich MN, Gambaryan AS. 2012. Solid-phase assays of receptor-binding specificity. Methods Mol Biol 865:71–94. https://doi.org/10.1007/978-1-61779-621-0_5.
25. Peng W, de Vries RP, Grant OC, Thompson AJ, McBride R, Tsogtbaatar B, Lee PS, Razi N, Wilson IA, Woods RJ, Paulson JC. 2017. Recent H3N2 viruses have evolved specificity for extended, branched human-type receptors, conferring potential for increased avidity. Cell Host Microbe 21:23–34. https://doi.org/10.1016/j.chom.2016.11.004.
26. Matrosovich MN, Gambaryan AS, Teneberg S, Piskarev VE, Yamnikova SS, Lvov DK, Robertson JS, Karlsson KA. 1997. Avian influenza A viruses differ from human viruses by recognition of sialyloligosaccharides and gangliosides and by a higher conservation of the HA receptor-binding site. Virology 233:224–234. https://doi.org/10.1006/viro.1997.8580.
27. Rogers GN, Paulson JC. 1983. Receptor determinants of human and animal influenza virus isolates: differences in receptor specificity of the H3 hemagglutinin based on species of origin. Virology 127:361–373. https://doi.org/10.1016/0042-6822(83)90150-2.
28. Yamada S, Suzuki Y, Suzuki T, Le MQ, Nidom CA, Sakai-Tagawa Y, Muramoto Y, Ito M, Kiso M, Horimoto T, Shinya K, Sawada T, Kiso M, Usui T, Murata T, Lin Y, Hay A, Haire LF, Stevens DJ, Russell RJ, Gamblin SJ, Skehel JJ, Kawaoka Y. 2006. Haemagglutinin mutations responsible for the binding of H5N1 influenza A viruses to human-type receptors. Nature 444:378–382. https://doi.org/10.1038/nature05264.
29. Gamblin SJ, Haire LF, Russell RJ, Stevens DJ, Xiao B, Ha Y, Vasisht N, Steinhauer DA, Daniels RS, Elliot A, Wiley DC, Skehel JJ. 2004. The structure and receptor binding properties of the 1918 influenza hemagglutinin. Science 303:1838–1842. https://doi.org/10.1126/science.1093155.
30. Rogers GN, Paulson JC, Daniels RS, Skehel JJ, Wilson IA, Wiley DC. 1983. Single amino acid substitutions in influenza haemagglutinin change receptor binding specificity. Nature 304:76–78. https://doi.org/10.1038/304076a0.
31. Wu NC, Thompson AJ, Xie J, Lin CW, Nycholat CM, Zhu X, Lerner RA, Paulson JC, Wilson IA. 2018. A complex epistatic network limits the mutational reversibility in the influenza hemagglutinin receptor-binding site. Nat Commun 9:1264. https://doi.org/10.1038/s41467-018-03663-5.
32. Lewis NS, Anderson TK, Kitikoon P, Skepner E, Burke DF, Vincent AL. 2014. Substitutions near the hemagglutinin receptor-binding site determine the antigenic evolution of influenza A H3N2 viruses in U.S. swine. J Virol 88:4752–4763. https://doi.org/10.1128/JVI.03805-13.
33. Petrova VN, Russell CA. 2018. The evolution of seasonal influenza viruses. Nat Rev Microbiol 16:47–60. https://doi.org/10.1038/nrmicro.2017.118.
34. Barr IG, Russell C, Besselaar TG, Cox NJ, Daniels RS, Donis R, Engelhardt OG, Grohmann G, Itamura S, Kelso A, McCauley J, Odagiri T, Schultz-Cherry S, Shu Y, Smith D, Tashiro M, Wang D, Webby R, Xu X, Ye Z, Zhang W, Writing Committee of the World Health Organization Consultation on Northern Hemisphere Influenza Vaccine Composition for 2013-2014. 2014. WHO recommendations for the viruses used in the 2013-2014 Northern Hemisphere influenza vaccine: epidemiology, antigenic and genetic characteristics of influenza A(H1N1)pdm09, A(H3N2) and B influenza viruses collected from October 2012 to January 2013. Vaccine 32:4713–4725. https://doi.org/10.1016/j.vaccine.2014.02.014.
35. Klimov AI, Garten R, Russell C, Barr IG, Besselaar TG, Daniels R, Engelhardt OG, Grohmann G, Itamura S, Kelso A, McCauley J, Odagiri T, Smith D, Tashiro M, Xu X, Webby R, Wang D, Ye Z, Yuelong S, Zhang W, Cox N. Writing Committee of the World Health Organization Consultation on Southern Hemisphere Influenza Vaccine Composition for 2013-2014. 2012. WHO recommendations for the viruses to be used in the 2012 Southern Hemisphere influenza vaccine: epidemiology, antigenic and genetic characteristics of influenza A(H1N1)pdm09, A(H3N2) and B influenza viruses collected from February to September 2011. Vaccine 30:6461–6471. https://doi.org/10.1016/j.vaccine.2012.07.089.
36. Govorkova EA, Matrosovich MN, Tuzikov AB, Bovin NV, Gerdil C, Fanget B, Webster RG. 1999. Selection of receptor-binding variants of human influenza A and B viruses in baby hamster kidney cells. Virology 262:31–38. https://doi.org/10.1006/viro.1999.9892.
37. Lin Y, Wharton SA, Whittaker L, Dai M, Ermetal B, Lo J, Pontoriero A, Baumeister E, Daniels RS, McCauley JW. 2017. The characteristics and antigenic properties of recently emerged subclade 3C.3a and 3C.2a human influenza A(H3N2) viruses passaged in MDCK cells. Influenza Other Respir Viruses 11:263–274. https://doi.org/10.1111/irv.12447.
38. Tamura D, Nguyen HT, Sleeman K, Levine M, Mishin VP, Yang H, Guo Z, Okomo-Adhiambo M, Xu X, Stevens J, Gubareva LV. 2013. Cell culture-selected substitutions in influenza A(H3N2) neuraminidase affect drug susceptibility assessment. Antimicrob Agents Chemother 57:6141–6146. https://doi.org/10.1128/AAC.01364-13.
39. Mohr PG, Deng YM, McKimm-Breschkin JL. 2015. The neuraminidases of MDCK grown human influenza A(H3N2) viruses isolated since 1994 can demonstrate receptor binding. Virol J 12:67. https://doi.org/10.1186/s12985-015-0295-3.
40. Zost SJ, Parkhouse K, Gumina ME, Kim K, Diaz Perez S, Wilson PC, Treanor JJ, Sant AJ, Cobey S, Hensley SE. 2017. Contemporary H3N2 influenza viruses have a glycosylation site that alters binding of antibodies elicited by egg-adapted vaccine strains. Proc Natl Acad Sci U S A 114:12578–12583. https://doi.org/10.1073/pnas.1712377114.
41. Aich U, Beckley N, Shriver Z, Raman R, Viswanathan K, Hobbie S, Sasisekharan R. 2011. Glycomics-based analysis of chicken red blood cells provides insight into the selectivity of the viral agglutination assay. FEBS J 278:1699–1712. https://doi.org/10.1111/j.1742-4658.2011.08096.x.
42. Das SR, Hensley SE, David A, Schmidt L, Gibbs JS, Puigbo P, Ince WL, Bennink JR, Yewdell JW. 2011. Fitness costs limit influenza A virus hemagglutinin glycosylation as an immune evasion strategy. Proc Natl Acad Sci U S A 108:E1417–E1422. https://doi.org/10.1073/pnas.1108754108.
43. Hensley SE, Das SR, Gibbs JS, Bailey AL, Schmidt LM, Bennink JR, Yewdell JW. 2011. Influenza A virus hemagglutinin antibody escape promotes neuraminidase antigenic variation and drug resistance. PLoS One 6:e15190. https://doi.org/10.1371/journal.pone.0015190.
44. Huang KY, Rijal P, Schimanski L, Powell TJ, Lin TY, McCauley JW, Daniels RS, Townsend AR. 2015. Focused antibody response to influenza linked to antigenic drift. J Clin Invest 125:2631–2645. https://doi.org/10.1172/JCI81104.
45. Stark SE, Caton AJ. 1991. Antibodies that are specific for a single amino acid interchange in a protein epitope use structurally distinct variable regions. J Exp Med 174:613–624. https://doi.org/10.1084/jem.174.3.613.
46. Ekiert DC, Kashyap AK, Steel J, Rubrum A, Bhabha G, Khayat R, Lee JH, Dillon MA, O'Neil RE, Faynboym AM, Horowitz M, Horowitz L, Ward AB, Palese P, Webby R, Lerner RA, Bhatt RR, Wilson IA. 2012. Cross-neutralization of influenza A viruses mediated by a single antibody loop. Nature 489:526–532. https://doi.org/10.1038/nature11414.
47. Pena L, Vincent AL, Ye J, Ciacci-Zanella JR, Angel M, Lorusso A, Gauger PC, Janke BH, Loving CL, Perez DR. 2011. Modifications in the polymerase genes of a swine-like triple-reassortant influenza virus to generate live attenuated vaccines against 2009 pandemic H1N1 viruses. J Virol 85:456–469. https://doi.org/10.1128/JVI.01503-10.
48. Tang Y, Lee CW, Zhang Y, Senne DA, Dearth R, Byrum B, Perez DR, Suarez DL, Saif YM. 2005. Isolation and characterization of H3N2 influenza A virus from turkeys. Avian Dis 49:207–213. https://doi.org/10.1637/7288-101304R.
49. Reed LJ, Muench H. 1938. A simple method for estimating fifty percent endpoints. Am J Hyg 27:493–497. https://doi.org/10.1093/oxfordjournals.aje.a118408.
50. Mena I, Nelson MI, Quezada-Monroy F, Dutta J, Cortes-Fernandez R, Lara-Puente JH, Castro-Peralta F, Cunha LF, Trovao NS, Lozano-Dubernard B, Rambaut A, van Bakel H, Garcia-Sastre A. 2016. Origins of the 2009 H1N1 influenza pandemic in swine in Mexico. Elife 5:e16777. https://doi.org/10.7554/eLife.16777.
51. Kearse M, Moir R, Wilson A, Stones-Havas S, Cheung M, Sturrock S, Buxton S, Cooper A, Markowitz S, Duran C, Thierer T, Ashton B, Meintjes P, Drummond A. 2012. Geneious Basic: an integrated and extendable desktop software platform for the organization and analysis of sequence data. Bioinformatics 28:1647–1649. https://doi.org/10.1093/bioinformatics/bts199.
52. Spackman E, Senne DA, Myers TJ, Bulaga LL, Garber LP, Perdue ML, Lohman K, Daum LT, Suarez DL. 2002. Development of a real-time reverse transcriptase PCR assay for type A influenza virus and the avian H5 and H7 hemagglutinin subtypes. J Clin Microbiol 40:3256–3260. https://doi.org/10.1128/JCM.40.9.3256-3260.2002.
53. Santos JJS, Obadan AO, Garcia SC, Carnaccini S, Kapczynski DR, Pantin-Jackwood M, Suarez DL, Perez DR. 2017. Short- and long-term protective efficacy against clade 2.3.4.4 H5N2 highly pathogenic avian influenza virus following prime-boost vaccination in turkeys. Vaccine 35:5637–5643. https://doi.org/10.1016/j.vaccine.2017.08.059.
54. World Health Organization. 2011. Manual for the laboratory diagnosis and virological surveillance of influenza. World Health Organization, Geneva, Switzerland.

55. Lakdawala SS, Lamirande EW, Suguitan AL, Jr, Wang W, Santos CP, Vogel L, Matsuoka Y, Lindsley WG, Jin H, Subbarao K. 2011. Eurasian-origin gene segments contribute to the transmissibility, aerosol release, and morphology of the 2009 pandemic H1N1 influenza virus. PLoS Pathog 7:e1002443. https://doi.org/10.1371/journal.ppat.1002443.
56. Stevens J, Chen L-M, Carney PJ, Garten R, Foust A, Le J, Pokorny BA, Manojkumar R, Silverman J, Devis R, Rhea K, Xu X, Bucher DJ, Paulson JC, Paulson J, Cox NJ, Klimov A, Donis RO. 2010. Receptor specificity of influenza A H3N2 viruses isolated in mammalian cells and embryonated chicken eggs. J Virol 84:8287–8299. https://doi.org/10.1128/JVI.00058-10.
57. Eswar N, Webb B, Marti-Renom MA, Madhusudhan MS, Eramian D, Shen MY, Pieper U, Sali A. 2006. Comparative protein structure modeling using Modeller. Curr Protoc Bioinformatics Chapter 5:Unit 5.6. https://doi.org/10.1002/0471250953.bi0506s15.
58. Schrodinger LLC. 2015. The PyMOL molecular graphics system, version 2.1. Schrodinger LLC, New York, NY.
59. Zhang Y, Aevermann BD, Anderson TK, Burke DF, Dauphin G, Gu Z, He S, Kumar S, Larsen CN, Lee AJ, Li X, Macken C, Mahaffey C, Pickett BE, Reardon B, Smith T, Stewart L, Suloway C, Sun G, Tong L, Vincent AL, Walters B, Zaremba S, Zhao H, Zhou L, Zmasek C, Klem EB, Scheuermann RH. 2017. Influenza Research Database: an integrated bioinformatics resource for influenza virus research. Nucleic Acids Res 45:D466–D474. https://doi.org/10.1093/nar/gkw857.